

# Chimera states on $m$ -directed hypergraphs

Rommel Tchinda Djeudjo,<sup>1,\*</sup> Timoteo Carletti,<sup>1</sup> Hiroya Nakao,<sup>2,3</sup> and Riccardo Muolo<sup>2,†</sup>

<sup>1</sup>*Department of Mathematics & naXys, Namur Institute for Complex Systems, University of Namur, B5000 Namur, Belgium*

<sup>2</sup>*Department of Systems and Control Engineering, Institute of Science Tokyo (former Tokyo Tech), Tokyo 152-8552, Japan*

<sup>3</sup>*International Research Frontiers Initiative, Institute of Science Tokyo (former Tokyo Tech), Kanagawa 226-8501, Japan*

(Dated: June 17, 2025)

Chimera states are synchronization patterns in which coherent and incoherent regions coexist in systems of identical oscillators. This elusive phenomenon has attracted a lot of interest and has been widely studied, revealing several types of chimeras. Most cases involve reciprocal pairwise couplings, where each oscillator exerts and receives the same interaction, modeled via networks. However, real-world systems often have non-reciprocal, non-pairwise (many-body) interactions. From previous studies, it is known that chimera states are more elusive in the presence of non-reciprocal pairwise interactions, while easier to be found when the latter are reciprocal and higher-order (many-body). In this work, we investigate the emergence of chimera states on non-reciprocal higher-order structures, called  $m$ -directed hypergraphs, and we show that, not only the higher-order topology allows the emergence of chimera states despite the non-reciprocal coupling, but also that chimera states can emerge because of the directionality. Finally, we compare the latter results with the one resulting from non-reciprocal pairwise interactions: their elusiveness confirms that the observed phenomenon is thus due to the presence of higher-order interactions. The nature of phase chimeras has been further validated through phase reduction theory.

## I. INTRODUCTION

Synchronization is a phenomenon observed in a wide variety of natural and engineered systems, ranging from flashing fireflies and cardiac pacemaker cells to power grids and neural circuits [1]. It arises when individual self-sustained oscillatory units adjust their rhythms due to their interactions, i.e., the coupling, which is often modeled through a network [2]. The structure of the interactions can lead to different kinds of synchronization patterns [3]. Among the most peculiar patterns of synchronization, one can find *chimera state*, a counterintuitive state in which coherent and incoherent behaviors coexist within the same system of identical oscillators. The phenomenon was first reported by Kaneko in the context of coupled maps [4, 5], and later observed in a variety of numerical studies involving both global, i.e., all-to-all [6–8] and nonlocal [9–13], i.e., first neighbors, coupling schemes. Despite these earlier observations, the scientific community nowadays acknowledges the seminal work by Kuramoto and Battogtokh [14] as the first systematic investigation and characterization of chimera states. This last work gained popularity after Abrams and Strogatz [15] coined the term “chimera” to describe the coexistence of different dynamical behaviors, inspired by the mythological creature composed of parts of different animals. Chimera states have also been identified in a range of experimental settings, lending credence to their physical relevance. These include Josephson junction arrays [16], electronic circuits [17, 18], lasers [19], mechanical oscillators [20], and nano-electromechanical systems [21]. Due to the elusive nature of chimera states, which are transient (for finite systems) and highly dependent on initial conditions, considerable effort has been devoted to identifying configurations,

e.g., specific ranges of parameters, coupling strengths, and network topologies, allowing the emergence and persistence of such patterns [22, 23]. Scholars have shown particular interest in the framework of neuroscience, where chimera-like patterns have been suggested as models for unihemispheric sleep observed in certain animals [24–26]. Since most real-world networks, including brain networks, are strongly non-reciprocal [27], the study of chimera states in the presence of non-reciprocal interactions becomes particularly relevant. However, except for a few works [28–33], the vast majority of the study on chimera states, including the references mentioned above, assumes reciprocal (i.e., symmetric) coupling.

Nonetheless, considering non-reciprocal interactions is only a first step towards more realistic settings. In fact, in recent years, more complex structures, such as hypergraphs and simplicial complexes, have triggered the interest of scholars and allowed to move beyond the network framework [34–40]. This is because networks, despite being a very good approximation, do not always fully capture the interactions in complex systems, which are often not only pairwise, i.e., one-by-one, but rather higher-order, i.e., group, interactions [34, 35]. Some examples are from neuroscience [41–44], ecology [45, 46], or social behaviors [47], to name a few. For what concerns the dynamics, higher-order interactions have been found to have great effects on the dynamics, for instance, in random walks [48, 49], synchronization [50–54], contagion [55, 56], or pattern formation [57, 58].

Chimera states have also been studied in presence of higher-order interactions, and it has been shown that they greatly enhance the emergence and persistence of various kinds of chimera state [59–63]. In this work, we go one step forward by considering non-reciprocal, i.e., directed, higher-order interactions, whose effects on the dynamics have been studied in the context of synchronization of chaotic oscillators [64, 65] and pattern formation [66]. In particular, we study the emergence of chimera states on  $m$ -directed hypergraphs [64] and show the emergence of amplitude mediated chimeras

\* rommel.tchindadjeudjo@unamur.be

† muolo.raa@m.titech.ac.jp

[67] and phase chimeras [68]. By comparing the results obtained on hypergraphs with those on networks, we can show that the observed patterns are caused by the higher-order interactions, which proves to be a strong driver for the presence of chimera states. Lastly, we further validate the analysis of phase chimera states through the phase reduction technique [69, 70].

In the next Section, we introduce  $m$ -directed hypergraphs, the dynamical model and some characterization tools for the chimera states. The results of amplitude mediated chimeras and phase chimeras, including the discussion on phase reduction, can be found, respectively, in Secs. III A and III B, right before the Conclusions.

## II. THE FRAMEWORK

In this Section, we first introduce the directed higher-order topology we will consider in our numerical study, together with its non-reciprocal pairwise counterpart; then, we present the model under study, the celebrated Stuart-Landau oscillator, and some quantities which are useful to characterize the kind of chimera state we are observing.

### A. $m$ -directed hypergraphs and clique-projected networks

A hypergraph is defined by the pair  $(V, E)$ , where  $V = \{v_1, v_2, \dots, v_N\}$  is a set of nodes (or vertices) and  $E = \{e_1, e_2, \dots, e_m\}$  is a set of hyperedges, each hyperedge being a subset of  $V$  containing at least two nodes. Note that a hyperedge composed of 2 nodes is a pairwise link, and that a hypergraph with only such hyperedges is a network. A hypergraph is said to be  $k$ -uniform when each hyperedge consists of  $k$  nodes, which is the kind we will consider throughout this work. Moreover, the higher-order structures we consider are non-reciprocal, namely,  $m$ -directed hypergraphs [64]. A hypergraph with a  $d$ -hyperedge, i.e., formed by  $d + 1$  nodes<sup>1</sup>, is said to be  $m$ -directed ( $m \leq d$ ) if the nodes can be split into two groups, one containing  $m$  head nodes and the second one the remaining  $q = d + 1 - m$  nodes, named tail nodes. The relevant fact is that each tail node influences each head node but the contrary is not necessarily true. On the other hand, head nodes interact among themselves. Note that this is a generalization of directed network, where there is one head node affected by one tail node through a directed link. In this case, the adjacency tensor becomes the adjacency matrix  $A_{i,j}$ , with the convention that it takes value 1 (or a positive real number, if the network is weighted) when there is a directed link from node  $j$  to node  $i$ , and 0 otherwise.

Let us consider a hyperedge consisting of the head group  $i_1, \dots, i_m$  and the tail group  $j_1, \dots, j_q$ ; because head nodes

interact with each other and nodes in the tail interact interchangeably with nodes in the head, the  $m$ -directed  $d$ -hyperedge,  $d = m + q - 1$ , has the following property

$$A_{\pi_1(i_1 \dots i_m) \pi_2(j_1 \dots j_q)}^{(d)} = 1, \quad (1)$$

where  $A^{(d)}$  is the  $d$ -th order adjacency tensor encoding  $(d + 1)$ -body interactions,  $\pi_1(i_1 \dots i_m)$  represents any permutation of the indices  $i_1, \dots, i_m$ , and  $\pi_2(j_1 j_2 j_3 \dots j_q)$  any permutation of the indices  $j_1, \dots, j_q$ . Note that the tensor can take a positive real value, in the case of weighted hypergraph.

In the present work, we consider the case of directed hyper-rings, which is a particular case of uniform hypergraph. An example of a symmetric 3-uniform 2-hypergraph is reported in Fig. 1, whereas in Fig. 2 we can appreciate a 3-uniform 1-directed 2-hypergraph built by “juxtaposing” three weighted 1-directed 2-hyperedges. Let us observe that the chosen structure allows us to have a rotation invariance, often used in models of chimera states on networks, and it is a possible generalization of a higher-order nonlocal coupling [62], although not the only one (see, for example, Refs. [61, 71, 72]). In the following we will denote by “junction” nodes those elements shared among two adjacent hyperedges.

The proposed construction allows to obtain a family of hypergraphs whose directionality can be controlled by tuning three parameters,  $q_1$ ,  $q_2$  and  $q_3$ . There are two methods of tuning the directionality [64]. The first one, named method (i), relies on fixing one weight, say  $q_1 = 1$ , and then changing the values of the remaining ones. For a 2-hypergraph, one can thus have

$$q_1 = 1, \quad q_2 = q_3 = p, \quad \text{with } p \in [0, 1].$$

This method does not conserve the total weight of the hyperedge and, thus, the (generalized weighted) degree is not preserved neither. An alternative method, called method (ii), consists in normalizing the parameters  $q_1 + q_2 + q_3 = 1$ , preserving thus the total weight of the hyperedge. For a 2-hypergraph, we have

$$q_1 = 1 - 2p, \quad q_2 = q_3 = p, \quad \text{with } p \in \left[0, \frac{1}{3}\right],$$

in such a way that a symmetric hypergraph can be recovered for  $p = 1/3$ . The results discussed in Section III are for method (i), but there is no qualitative difference when we use method (ii) to tune the directionality.

Lastly, let us introduce a network obtained from the directed hypergraph, that will be used as benchmark to test the emergence of chimera states in comparison to the higher-order case. We thus propose a directed clique-projected network obtained by adding a directed link between nodes in the tail of the hyperedge and nodes in the head of the hyperedges. Nodes in the head will also be connected among themselves via symmetric links. Note that, in general, the resulting directed clique projected network will be weighted. In Fig. 3 we report a simple example of such structure.

<sup>1</sup> Note that in some earlier works on hypergraphs, a  $d$ -hyperedge encodes a  $d$ -body interaction, while we follow the more common terminology, consistent with the literature on simplicial complexes, where a  $d$ -simplex encodes  $(d + 1)$ -body interactions [36].

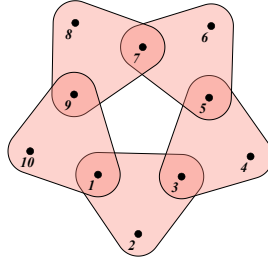


Figure 1. A 2-hyperring made of hyperedges and 10 nodes.

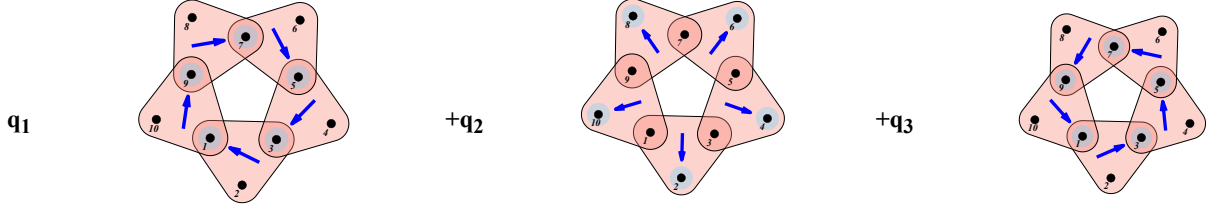


Figure 2. We schematically represent a family of **1-directed 2-hyperrings** obtained as a weighted “combination” of three base hyperrings. Each hyperring is made of 1-directed 2-hyperedges, weighted by the coefficients  $(q_1, q_2, q_3)$ . When  $q_1 = q_2 = q_3 = 1$ , the resulting structure is a **symmetric 2-hyperring**, as shown in Fig. 1. On the other hand, different weights allow to generate a family of **1-directed 2-hyperrings**, where some directions are favored. The heads of the hyperedges are highlighted in light blue, while arrows help to identify the directionality of the hyperedges, illustrating thus the direction of the interactions in the hyperring. In Appendix B, we show an analogous construction for the case of **2-directed 2-hyperrings**.

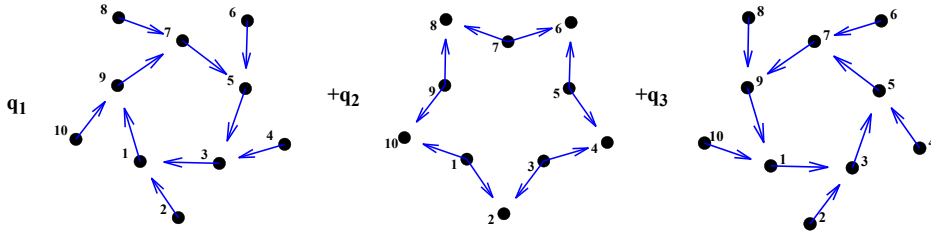


Figure 3. We schematically represent a family of clique-projected networks, obtained from the 1-directed 2-hyperring presented in Fig. 2. Each directed clique is obtained from the directed hyperedge and it is weighted by the coefficients  $(q_1, q_2, q_3)$ . When  $q_1 = q_2 = q_3 = 1$ , the resulting structure is a symmetric network.

## B. Stuart-Landau oscillators

Let us now consider  $N$  identical nonlinear systems coupled via a 1-directed hypergraph of order  $D$ , with  $D \geq 2$ . Because of the presence of a single node in the head, we will denote the  $d$ -hyperedge by  $A_{ij_1 \dots j_d}^{(d)}$ . The dynamics is given by the following set of equations

$$\dot{x}_i = f(x_i) + \sum_{d=1}^D \sigma_d \sum_{j_1, \dots, j_d=1}^N A_{ij_1 j_2 \dots j_d}^{(d)} g^{(d)}(x_i, x_{j_1}, \dots, x_{j_d}), \quad (2)$$

where, for all  $i = 1, \dots, N$ ,  $x_i \in \mathbb{R}^m$  denotes the state vector describing the dynamics of the  $i$ -th oscillator,  $f : \mathbb{R}^m \rightarrow \mathbb{R}^m$  is the nonlinear function determining the evolution of the system, and  $g^{(d)} : \mathbb{R}^{m \times (d+1)} \rightarrow \mathbb{R}^m$  represents the nonlinear function responsible for the coupling among nodes in the same hyperedge. Note that, for us  $m = 2$ , as the system introduced

below has such dimensionality. We hereby assume the coupling to be diffusive-like, namely

$$g^{(d)}(x_i, x_{j_1}, \dots, x_{j_d}) = h^{(d)}(x_{j_1}, x_{j_2}, \dots, x_{j_d}) - h^{(d)}(x_i, x_i, \dots, x_i), \quad (3)$$

where  $h^{(d)} : \mathbb{R}^{m \times d} \rightarrow \mathbb{R}^m$ . Then, the previous equations of motion become

$$\dot{x}_i = f(x_i) + \sum_{d=1}^D \sigma_d \sum_{j_1, j_2, \dots, j_d=1}^N A_{ij_1 j_2 \dots j_d}^{(d)} \times \left[ h^{(d)}(x_{j_1}, x_{j_2}, \dots, x_{j_d}) - h^{(d)}(x_i, x_i, \dots, x_i) \right], \quad (4)$$

with  $A_{i\pi_2(j_1 \dots j_d)}^{(d)}$  keeping the same value for any permutation  $\pi_2$ , the hypergraph being 1-directed. In the case of 1-directed 2-hyperrings, the coupling functions are chosen to be

$$h^{(2)}(x_{j_1}, x_{j_2}) = x_{j_1}^2 x_{j_2} \quad \text{and} \quad h^{(2)}(x_i, x_i) = x_i^3. \quad (5)$$

We consider a system made of  $N$  interacting Stuart-Landau units, a paradigmatic model in the study of synchronization dynamics, as it corresponds to the normal form of the supercritical Hopf-Andronov bifurcation [73]. With the coupling as above, the equations read

$$\begin{cases} \frac{dx_i}{dt} = \alpha x_i - \omega y_i - (x_i^2 + y_i^2)x_i + \varepsilon \sum_{j_1, \dots, j_2} A_{i, j_1, j_2}^{(1)} (x_{j_1}^2 x_{j_2} - x_i^3), \\ \frac{dy_i}{dt} = \omega x_i + \alpha y_i - (x_i^2 + y_i^2)y_i + \varepsilon \sum_{j_1, \dots, j_2} A_{i, j_1, j_2}^{(1)} (x_{j_1}^2 x_{j_2} - x_i^3), \end{cases} \quad (6)$$

where  $\alpha$  is a bifurcation parameter and  $\omega$  is the frequency of the oscillators. Note that the coupling follows the configuration  $x \rightarrow x, y \rightarrow x$ , as in previous works [18, 62, 63]. Let us observe that units are identical, namely the parameters  $\alpha$  and  $\omega$  are the same for every unit in the system. Each isolated system exhibits a stable limit cycle for  $\alpha > 0$ , condition that we assume true throughout this study.

The dynamics of corresponding system on the clique-projected network is given by

$$\begin{cases} \dot{x}_i = \alpha x_i - \omega y_i - (x_i^2 + y_i^2)x_i + \varepsilon \sum_{j=1}^N A_{i,j} (x_j^3 - x_i^3), \\ \dot{y}_i = \omega x_i + \alpha y_i - (x_i^2 + y_i^2)y_i + \varepsilon \sum_{j=1}^N A_{i,j} (x_j^3 - x_i^3). \end{cases}$$

### C. Frequency, phase, and amplitude

Before presenting the results, let us introduce the quantities we will use to characterize chimera states. After a transient interval and for a given time window, the orbit of the  $i$ -th oscillator can be written as  $a_i(t) \exp[i(2\pi\Omega_i t + \theta_i)]$ , where  $i$  is the imaginary unit,  $a_i(t)$  is the amplitude of the oscillations,  $\Omega_i$  its frequency, and  $\phi_i = 2\pi\Omega_i t + \theta_i$  its phase. To be more precise,  $\omega = 2\pi\Omega$  is the *angular frequency*, whilst  $\Omega$  is the properly called *frequency*; in what follows we will call them both "frequency", as we believe that there is no ambiguity and it is clear what they mean. When the chimera behavior, i.e., the coexistence of coherence and incoherence, is relative to amplitude and this induces a chimera behavior also on the phase, we talk about **amplitude mediated chimeras** [67]. When the chimera behavior is only with respect to the phase, while amplitudes and frequencies are constant, then we are dealing with **phase chimeras** [68]. These are the two phenomenologies that we have observed in the performed numerical study.

## III. RESULTS

The aim of this section is to present our main results obtained by numerically integrating Eqs. (6) starting from clustered initial conditions,  $x_i = 1, y_i = -1$  for  $i \in [1, N/2]$ , and  $x_i = -1, y_i = 1$  for  $i \in [N/2 + 1, N]$ . In what follows, we will vary the directionality of the hyperedges by using the

method not preserving the coupling strength of the hyperedge (i.e., method (i) of the previous Section). We will fix a privileged direction by setting  $q_1 = 1$  and then uniformly vary  $q_2 = q_3 = p$ . When  $p = 1$ , the hypergraph is symmetric, while the asymmetry is introduced when  $1 > p \geq 0$ . The results obtained with method (ii) show no significant difference, hence, we will not show them. In the appendices, we show additional results for a different orientation of 1-directed 2-hyperring (Appendix A) and for 2-directed 2-hyperrings (Appendix B).

### A. Amplitude mediated chimera states

Let us first consider a configuration in which no chimera is observed when the topology is symmetric. In Fig. 4 we show the effect of the directionality, tuned by the parameter  $p$ . The reported results demonstrate that intermediate values of  $p$  can promote the emergence of chimera states, namely, **amplitude mediated chimeras**. Moreover, such patterns are not stationary, thus they are traveling amplitude mediated chimeras. Starting with  $p = 1$ , i.e., symmetric case (leftmost column), we observe a coherent behavior in the whole system (top row), where all oscillators have the same constant amplitude  $a_i$  (second row from the top), same constant frequency  $\Omega_i$  (third row from the top) and coherent phases,  $\theta_i$  (bottom row). By decreasing  $p$  (namely, from  $p \lesssim 0.45$ ), i.e., by increasing the directionality, the system tends to favor the formation of complex dynamical patterns (see the second and the third columns from the left in Fig. 4). In particular, let us emphasize the amplitudes distributed in two groups, one for which  $a_i$  are very close to 1 and the remaining ones whose amplitudes are distributed in (0.5, 1). This observation highlights the critical role of directionality in determining the nature of interesting emergent states, where localized coherence and incoherence can coexist. Let us, however, observe that when the directionality is maximal, namely  $p = 0$  (rightmost column), the chimera pattern vanishes, as it can be appreciated by looking at the rightmost column of Fig. 4. This fact can be explained by observing that, once  $p = 0$ , because of the used regular structure, two types of nodes emerge: isolated nodes (non-junction nodes in this case) and non-isolated nodes (junction nodes). Each node in the former group oscillates on its own without receiving any input from any other node, meaning they act as "external pacemakers" towards nodes in the second group. The nodes of the first group, being isolated oscillators, follow their limit cycle solution with constant amplitude (see blue dots in panel d2), constant frequency (see blue dots in panel d3) and phases  $\theta_i$  reminiscent of the initial conditions (see blue dots in panel d4). Non-isolated nodes are constantly driven by the isolated ones and are not able to settle on any regular behavior; the amplitudes are close but irregularly distributed among the nodes (see red dots in panel d2), the frequencies are constant but slightly different from the one of the limit cycle (see red dots in panel d3), and, finally, the phases are randomly scattered in  $(-\pi, \pi)$  (see red dots in panel d4).

To test the role of higher-order interactions in the emergence of this behavior, we compared the previous results with

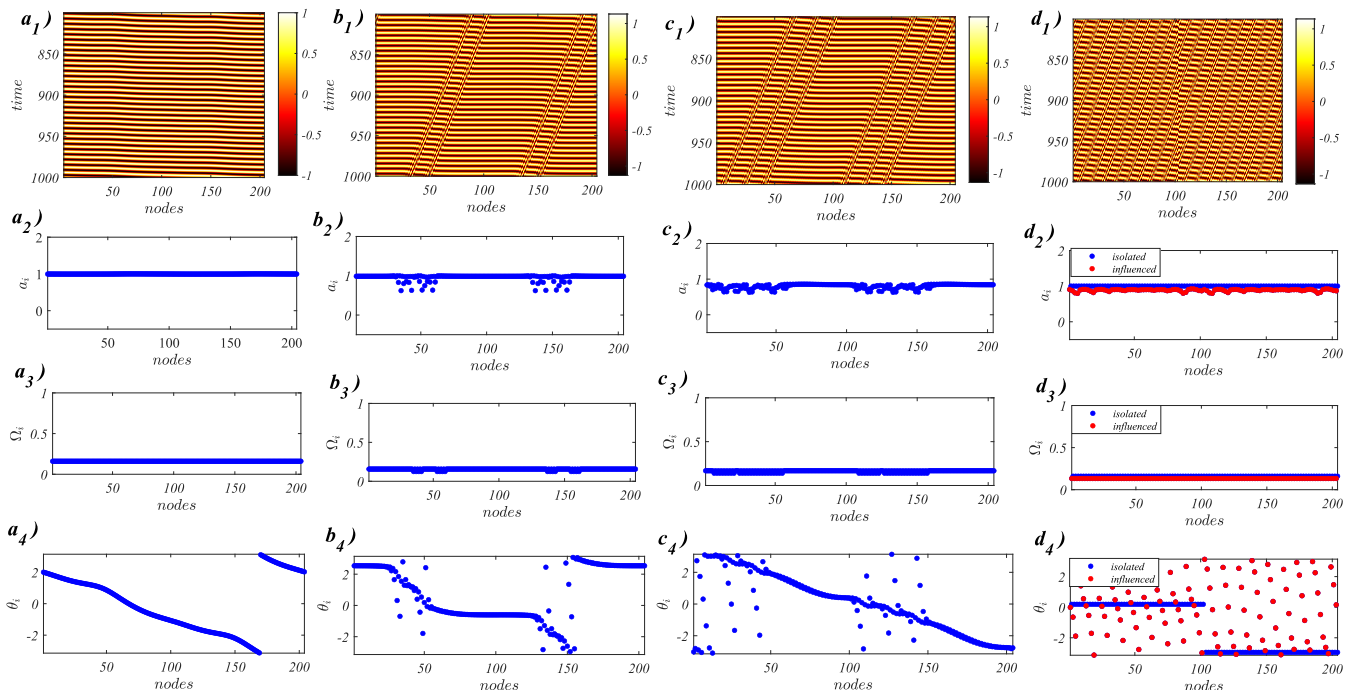


Figure 4. Analysis of the dynamics on a 1-directed 2-hyperring of 204 nodes. The first row shows the spatiotemporal diagrams, the second row the amplitudes, the third row the frequencies, and the last row the phases. The directionality parameter  $p$  is varied with the columns: (a1, a2, a3, a4) coherent behavior for  $p = 1$ ; (b1, b2, b3, b4) traveling amplitude mediated chimera state for  $p = 0.2$ ; (c1, c2, c3, c4) traveling amplitude mediated chimera state for  $p = 0.1$ ; (d1, d2, d3, d4) incoherent behavior for  $p = 0$ . The model parameters are  $\alpha = 1$  and  $\omega = 1$ , and the coupling strength is  $\varepsilon = 0.2$ .

the case of directed clique-projected networks. We thus numerically solved system (7) by using the same initial conditions, coupling strength, parameters and directionality tuning as above. The results are reported in Fig. 5 and show a different behavior. In the symmetric case, i.e.,  $p = 1$ , (leftmost column) and with  $p = 0.2$  (second column from the left), the system exhibits a coherent behavior. For  $p = 0.1$  (second column from the right), **phase chimeras** appear; nonetheless, the incoherent region is small if compared to the same obtained in presence of many-body interactions. In particular, no traveling patterns are observed whatsoever. Finally, for  $p = 0$  (rightmost column), we have isolated (pacemakers-like) and non-isolated nodes, and the behavior is analogous to what is observed in the higher-order case.

The chimera patterns observed in this setting are interesting because they are caused by the combination of higher-order interactions and directionality. For high-directionality (i.e., low values of  $p$ ) some kind of pattern would be expected, as the non-isolated nodes are forced oscillators, a setting that is known to give rise to chimeras [33]. However, thanks to the presence of higher order interactions, chimera states are observed also for intermediate values of directionality.

## B. Phase chimera states

We now consider the same setting as before, but for a much smaller value of the coupling strength. In the higher-order set-

ting, the symmetric case already exhibits phase chimeras, i.e., the oscillators have (almost) identical amplitudes,  $a_i \sim 1$  and identical frequencies  $\Omega_i$ , while we can observe the presence of coherent and incoherent domains for the phases  $\theta_i$ . The results are reported in Fig. 6. It is interesting to see that the chimera behavior persists when the directionality is introduced.

When we compare those results with the pairwise case, i.e., clique-projected network, we see that only for high directionality (i.e., small values of  $p$ ) we appreciate some kind of phase chimera behavior, but the region of incoherence is smaller.

As for the case of the previous section, some kind of patterns for high directionality would be expected. What is interesting is that the phase chimera behavior is conserved from the symmetric to the fully asymmetric case, which is due to the presence of higher-order interactions.

## C. Validation through phase reduction theory

The patterns observed in the previous Section are phase chimeras and are characterized by (almost) constant amplitudes. Hence, they should be also observed in a “pure” phase model, i.e., where amplitudes do not play any role. To validate this claim, we apply the phase reduction method [69, 70] to the Stuart-Landau oscillators. The main idea behind the phase reduction method consists of reducing a given oscillatory system to a phase model, i.e., Kuramoto-type [74–76]. Very briefly (see [69] for a tutorial), starting from a system of

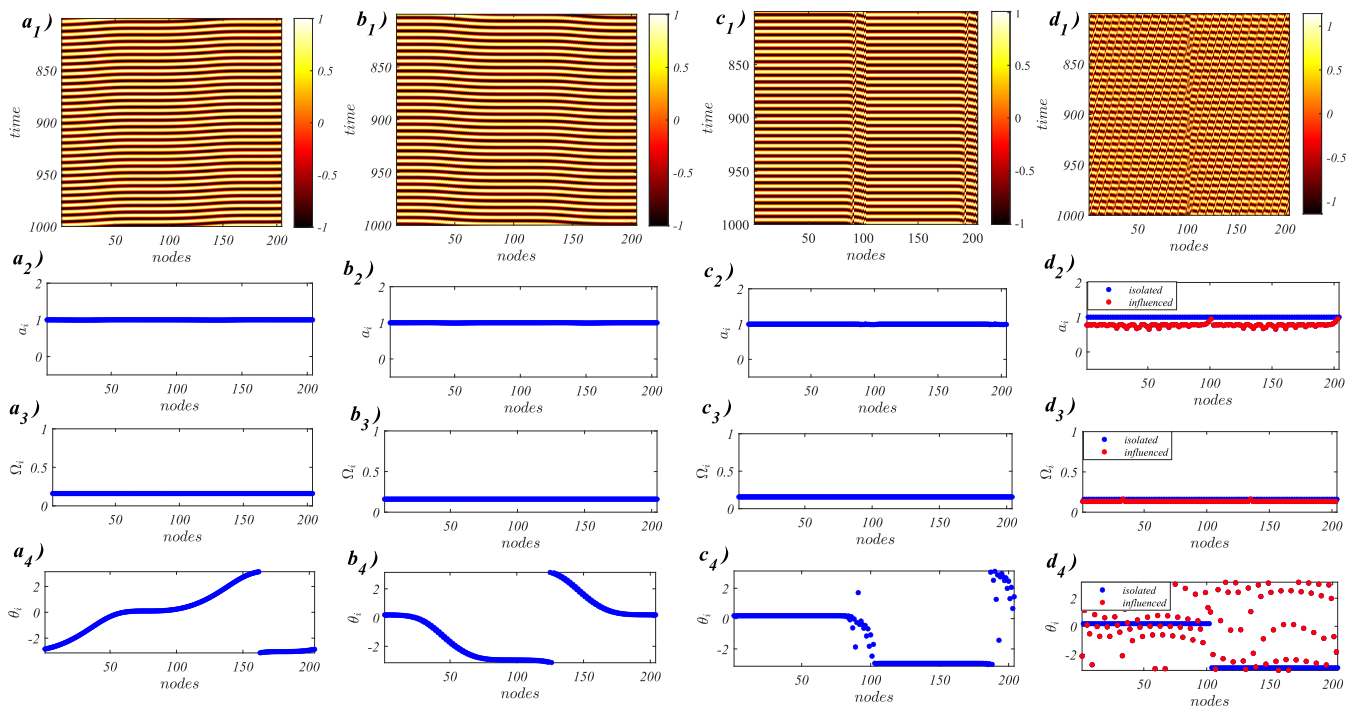


Figure 5. Analysis of the dynamics on a clique-projected network of 204 nodes. The first row shows the spatiotemporal diagrams, the second row the amplitudes, the third row the frequencies, and the last row the phases. The directionality parameter  $p$  is varied with the columns: (a1, a2, a3, a4) coherent behavior for  $p = 1$ ; (b1, b2, b3, b4) coherent behavior for  $p = 0.2$ ; (c1, c2, c3, c4) phase chimera state for  $p = 0.1$ ; (d1, d2, d3, d4) incoherent behavior for  $p = 0$ . The model parameters are  $\alpha = 1$  and  $\omega = 1$ , and the coupling strength is  $\varepsilon = 0.2$ .

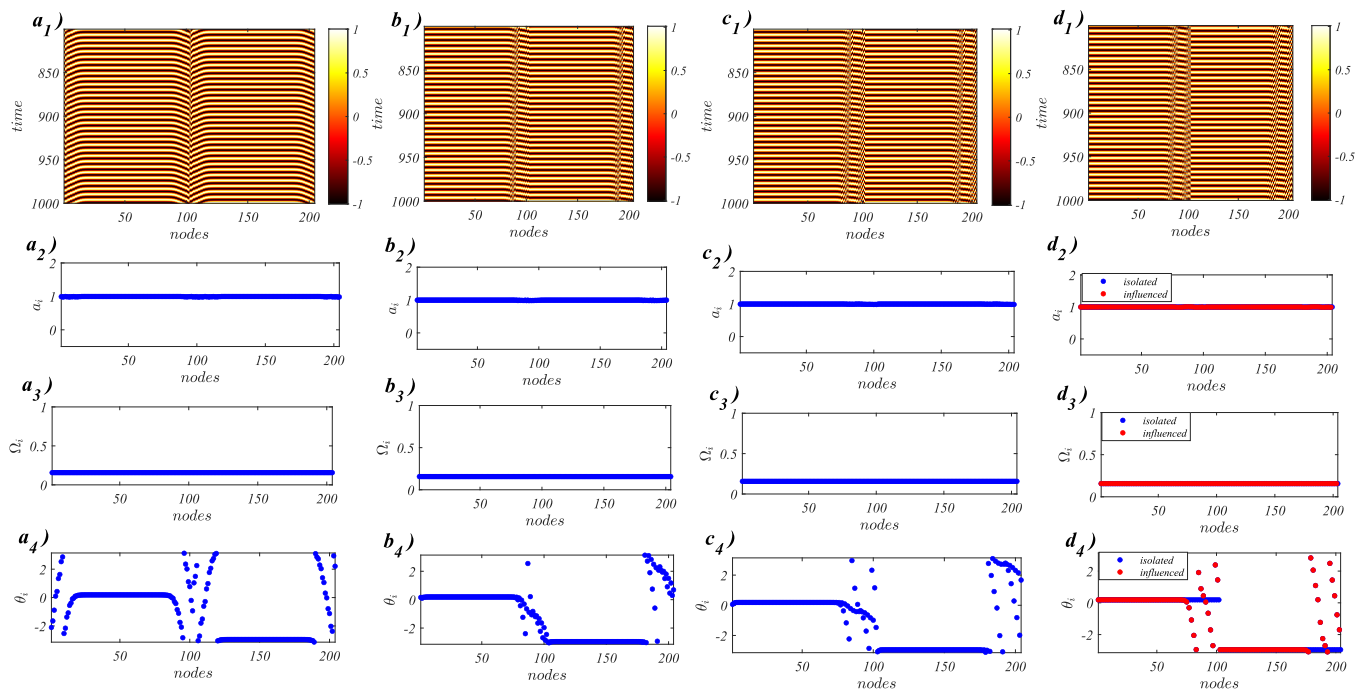


Figure 6. Analysis of the dynamics on a 1-directed 2-hyperring of 204 nodes. The first row shows the spatiotemporal diagrams, the second row the amplitudes, the third row the frequencies, and the last row the phases. The directionality parameter  $p$  is varied with the columns: (a1, a2, a3, a4) phase chimera state for  $p = 1$ ; (b1, b2, b3, b4) phase chimera state for  $p = 0.2$ ; (c1, c2, c3, c4) phase chimera state for  $p = 0.1$ ; (d1, d2, d3, d4) phase chimera state for  $p = 0$ . The model parameters are  $\alpha = 1$  and  $\omega = 1$ , and the coupling strength is  $\varepsilon = 0.015$ .

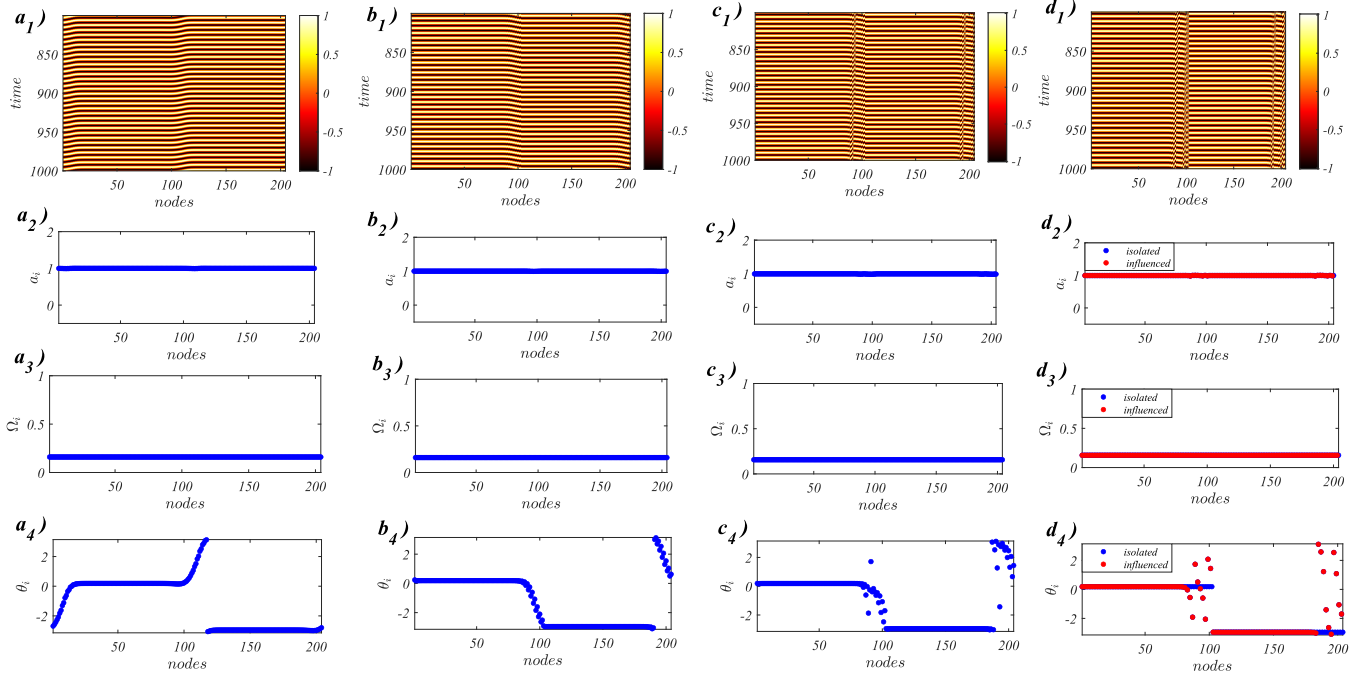


Figure 7. Analysis of the dynamics on a clique-projected network of 204 nodes. The first row shows the spatiotemporal diagrams, the second row the amplitudes, the third row the frequencies, and the last row the phases. The directionality parameter  $p$  is varied with the columns: (a1, a2, a3, a4) coherent clusters for  $p = 1$  ; (b1, b2, b3, b4) coherent clusters for  $p = 0.2$  ; (c1, c2, c3, c4) phase chimera state for  $p = 0.1$  ; (d1, d2, d3, d4) phase chimera state for  $p = 0$ . The model parameters are  $\alpha = 1$  and  $\omega = 1$ , and the coupling strength is  $\varepsilon = 0.0015$ .

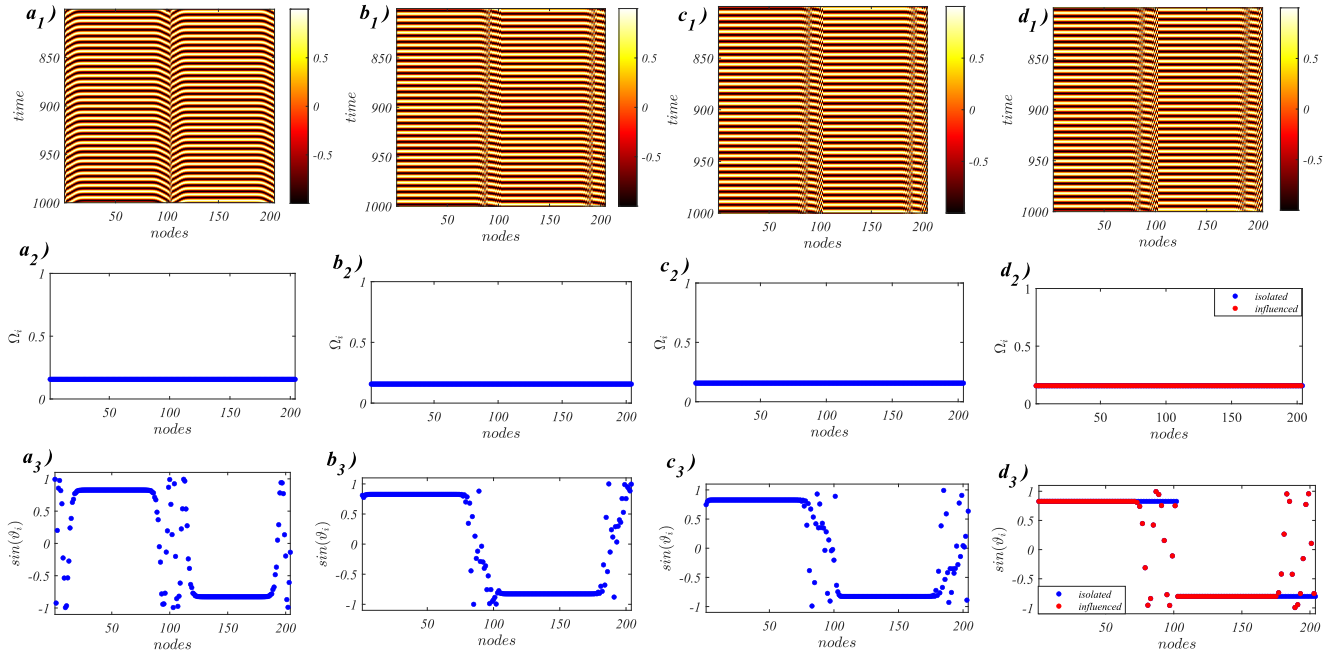


Figure 8. Analysis of the dynamics of the phase reduced model on a 1-directed 2-hypergraph of 204 nodes. The first row shows the spatiotemporal diagrams, the second row the frequencies, and the last row the phases. The directionality parameter  $p$  is varied with the columns: (a1, a2, a3) phase chimera states for  $p = 1$  ; (b1, b2, b3) phase chimera states for  $p = 0.2$  ; (c1, c2, c3) phase chimera states for  $p = 0.1$  ; (d1, d2, d3) phase chimera states for  $p = 0$ . The coupling strength is  $\varepsilon = 0.015$  and the (angular) frequency is  $\omega = 1$ .

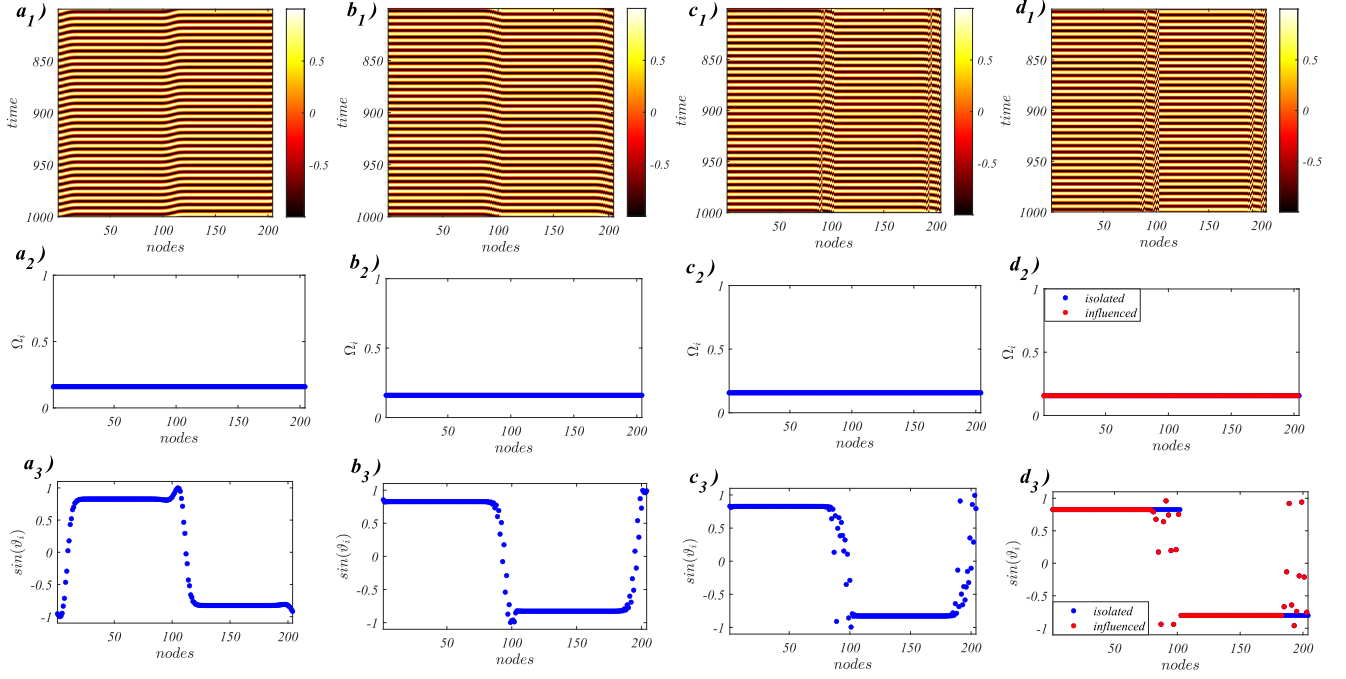


Figure 9. Analysis of the dynamics of the phase reduced model on a clique-projected network of 204 nodes. The first row shows the spatiotemporal diagrams, the second row the frequencies, and the last row the phases. The directionality parameter  $p$  is varied with the columns: (a1, a2, a3) coherent clusters for  $p = 1$ ; (b1, b2, b3) coherent clusters for  $p = 0.2$ ; (c1, c2, c3) phase chimera states for  $p = 0.1$ ; (d1, d2, d3) phase chimera states for  $p = 0$ . The coupling strength is  $\varepsilon = 0.015$  and the (angular) frequency is  $\omega = 1$ .

identical<sup>2</sup> weakly coupled self-sustained oscillators, e.g.,

$$\dot{\vec{X}}_i = \vec{F}(\vec{X}_i) + \varepsilon \sum_{j=1}^N A_{ij} \vec{G}_{ij}(\vec{X}_j, \vec{X}_i), \quad (7)$$

the system can be reduced to the sole phase equations, i.e.,

$$\dot{\vartheta}_i = \omega + \varepsilon \sum_{j=1}^N A_{ij} \vec{Z}(\vartheta_i) \cdot \vec{G}_{ij}(\vartheta_j, \vartheta_i), \quad (8)$$

where  $\omega$  is the frequency of the  $i$ -th oscillator and  $\vec{Z}$  is the phase sensitivity function, whose expression can be obtained analytically only for Stuart-Landau [69] and weakly nonlinear oscillators [77]. The phase reduction theory has been recently applied to systems with higher-order interactions [63, 78–

82], allowing to obtain higher-order versions of the Kuramoto model<sup>3</sup>.

By using the phase sensitivity function for the SL oscillator, i.e.,  $\vec{Z}(\vartheta) = (-\sin \vartheta, \cos \vartheta)^T$  and by expressing the vector field in polar coordinates remembering that,  $\alpha$  being 1, the amplitude of the limit cycle is 1,  $\vec{X}_i = (\cos \vartheta_i, \sin \vartheta_i)^T$ , we can apply the phase reduction method, obtaining the following equation for the phases

$$\frac{d\vartheta_i}{dt} = \omega + \varepsilon \sum_{j_1, j_2} A_{i, j_1, j_2} \Phi(\vartheta_i, \vartheta_{j_1}, \vartheta_{j_2}), \quad (9)$$

where  $\omega$  is the natural frequency and  $\Phi$  is a coupling function dependent on phase differences. Note that, because of our choice of parameters in the Stuart-Landau, the variable  $\omega$  corresponds to the frequency of both models. By applying the averaging method over one oscillation period [85], for the case of 2-hyperring with cubic coupling, the coupling function  $\Phi$  can be explicitly computed as

$$\Phi(\vartheta_i, \vartheta_{j_1}, \vartheta_{j_2}) = \frac{1}{4} \cos(\vartheta_{j_2} - \vartheta_i) + \frac{1}{4} \sin(\vartheta_{j_2} - \vartheta_i) + \frac{1}{8} \cos(2\vartheta_{j_1} - \vartheta_{j_2} - \vartheta_i) + \frac{1}{8} \sin(2\vartheta_{j_1} - \vartheta_{j_2} - \vartheta_i) - \frac{3}{8}.$$

<sup>2</sup> Note that the general theory works also for the case of non-identical oscillators, as long as the differences are small, namely, the frequency of each oscillator  $i$  is such that  $\omega_i = \omega + \delta\omega_i$ , with  $\delta\omega_i \ll 1$ .

<sup>3</sup> Note that there are several versions of the higher-order Kuramoto model not obtained through phase reductions, e.g., [50, 51, 83, 84]

Thus, the general model, after phase reduction in the case of

$$\frac{d\vartheta_i}{dt} = \omega + \varepsilon \sum_{j_1, j_2} A_{i, j_1, j_2} \left[ \frac{1}{4} \cos(\vartheta_{j_2} - \vartheta_i) + \frac{1}{4} \sin(\vartheta_{j_2} - \vartheta_i) + \frac{1}{8} \cos(2\vartheta_{j_1} - \vartheta_{j_2} - \vartheta_i) + \frac{1}{8} \sin(2\vartheta_{j_1} - \vartheta_{j_2} - \vartheta_i) - \frac{3}{8} \right]. \quad (10)$$

Let us observe that both pairwise and higher-order interactions are present in the phase model.

The same procedure can be repeated for the pairwise system, by obtaining

$$\dot{\vartheta}_i = \omega + \varepsilon \sum_{j=1}^N A_{ij} \psi(\vartheta_i, \vartheta_j), \quad (11)$$

where the coupling function  $\psi$  dependent on phase differences. Again, through averaging, we obtain the equations for the evolution of the phases

$$\dot{\vartheta}_i = \omega + \varepsilon \sum_{j=1}^N A_{ij} \frac{3}{8} \left[ \cos(\vartheta_j - \vartheta_i) + \sin(\vartheta_j - \vartheta_i) - 1 \right], \quad (12)$$

which is the well-known Kuramoto-Sakaguchi model [86].

We can now repeat the numerical analysis for the reduced models. The results presented in Fig. 8 refer to the dynamics on the 1-directed 2-hypergraph, while Fig. 9 shows the case of the clique-projected network. In both cases, the phase model behaves as the non-reduced model, confirming that the observed patterns are indeed phase chimera states.

#### IV. CONCLUSION

In this work, we have studied the emergence of chimera states in systems of oscillators coupled via directed hypergraphs. We have observed amplitude-mediated chimeras, which are clearly induced by the directionality, as no analogous effect was found on symmetric hypergraphs. Moreover, we have shown that phase chimera states observed on symmetric hypergraphs are preserved when directionality is induced. Both phenomena are higher-order effects, as the corresponding pairwise settings show either weak or no chimera at all. The nature of phase chimeras was further validated through phase reduction theory, a perturbative technique allowing to describe any limit cycle oscillator through a phase equation. The phase model obtained this way showed an analogous chimera pattern, confirming that had been observed is a phase chimera. While the dynamics we considered is general

the 2-hypergraph, is given by the following

and valid for any oscillatory system undergoing a supercritical Hopf-Andronov bifurcation, our hypergraph model remains a toy model. However, given that real-world interactions, especially those in the brain, are in general non-reciprocal and higher-order, this work makes a step forward towards more realistic settings in which chimera states can emerge.

#### ACKNOWLEDGEMENTS

H.N. acknowledges JSPS KAKENHI 25H01468, 25K03081, and 22H00516 for financial support. The work of R.M. is supported by a JSPS postdoctoral fellowship, grant 24KF0211.

#### Appendix A: 1-directed hypergraphs with different orientation

In this section, we also consider a different orientation of the 1-directed 2-hypergraph, namely,  $q_2 = 1$ , and  $q_1 = q_3 = p$ , so that the directionality is towards nodes that are not junction nodes. Also in this setting, we can obtain amplitude mediated chimeras (not traveling), shown in Fig. A1, and phase chimeras, shown in Fig. A2. Such states are not observed for the corresponding clique-projected network (results not shown).

#### Appendix B: 2-directed hypergraphs

If we now consider 2 nodes in the head of a directed hypergraph and 1 node in the tail, we obtain a 2-directed 2-hypergraph, as represented in Fig. B1. As for the case of 1-directed, we can easily obtain its corresponding clique-projected network, shown in Fig. B2. If we start from the same setting of Fig. 6 where the symmetric case exhibits phase chimeras, we see that such pattern is not conserved when inducing the directionality, as shown in Fig. B3. In fact, already from  $p \lesssim 0.9$  the phase chimera vanishes. In Fig. B4, we show the results for the clique-projected network, where no patterns are observed. Interestingly, there are no patterns even when the directionality is such that there are isolated nodes, at contrast with the case of the Main Text.

[1] A. Pikovsky, J. Kurths, and M. Rosenblum, *Synchronization: a universal concept in nonlinear sciences*, Vol. 12 (Cambridge university press, 2001).

[2] A. Arenas, A. Díaz-Guilera, J. Kurths, Y. Moreno, and C. Zhou, "Synchronization in complex networks," *Phys. Rep.* **469**, 93–153 (2008).

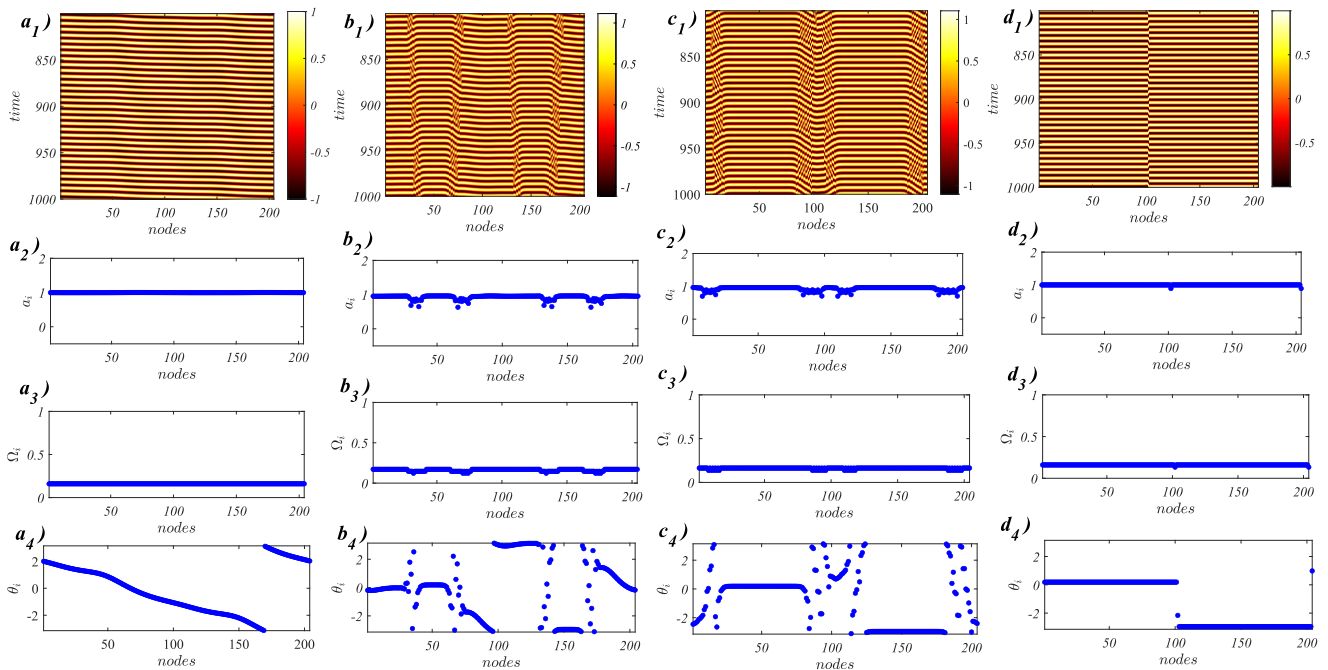


Figure A1. Analysis of the dynamics on a 1-directed 2-hyperring of 204 nodes with a different orientation with respect to the Main Text. The first row shows the spatiotemporal diagrams, the second row the amplitudes, the third row the frequencies, and the last row the phases. The directionality parameter  $p$  is varied with the columns: (a1, a2, a3, a4) coherent behavior for  $p = 1$ ; (b1, b2, b3, b4) amplitude mediated chimera state for  $p = 0.2$ ; (c1, c2, c3, c4) amplitude mediated chimera states for  $p = 0.1$ ; (d1, d2, d3, d4) coherent clusters for  $p = 0$ . The model parameters are  $\alpha = 1$  and  $\omega = 1$ , and the coupling strength is  $\varepsilon = 0.2$ .

- [3] S. Boccaletti, V. Latora, Y. Moreno, M. Chavez, and D.-U. Hwang, “Complex networks: Structure and dynamics,” *Phys. Rep.* **424**, 175–308 (2006).
- [4] Kunihiro Kaneko, “Period-doubling of kink-antikink patterns, quasiperiodicity in antiferro-like structures and spatial intermittency in coupled logistic lattice: towards a prelude of a “field theory of chaos”,” *Progress of Theoretical Physics* **72**, 480–486 (1984).
- [5] K. Kaneko, “Clustering, coding, switching, hierarchical ordering, and control in a network of chaotic elements,” *Physica D* **41**, 137–172 (1990).
- [6] Vincent Hakim and Wouter-Jan Rappel, “Dynamics of the globally coupled complex ginzburg-landau equation,” *Physical Review A* **46**, R7347 (1992).
- [7] N. Nakagawa and Y. Kuramoto, “Collective chaos in a population of globally coupled oscillators,” *Progress of Theoretical Physics* **89**, 313–323 (1993).
- [8] M.L. Chabanol, V. Hakim, and W.J. Rappel, “Collective chaos and noise in the globally coupled complex ginzburg-landau equation,” *Physica D: Nonlinear Phenomena* **103**, 273–293 (1997).
- [9] Y. Kuramoto, “Scaling behavior of turbulent oscillators with non-local interaction,” *Prog. Theor. Phys.* **94** (1995).
- [10] Y. Kuramoto and H. Nakao, “Origin of power-law spatial correlations in distributed oscillators and maps with nonlocal coupling,” *Phys. Rev. Lett.* **76** (1996).
- [11] Y. Kuramoto and H. Nakao, “Power-law spatial correlations and the onset of individual motions in self-oscillatory media with non-local coupling,” *Physica D* **103** (1997).
- [12] Y. Kuramoto, D. Battogtokh, and H. Nakao, “Multiaffine chemical turbulence,” *Phys. Rev. Lett.* **81** (1998).
- [13] Y. Kuramoto, H. Nakao, and D. Battogtokh, “Multi-scaled turbulence in large populations of oscillators in a diffusive medium,” *Physica A* **288** (2000).
- [14] Y. Kuramoto and D. Battogtokh, “Coexistence of coherence and incoherence in nonlocally coupled phase oscillators,” *Nonlinear Phenom. Complex Syst.* **5** (2002).
- [15] D.M. Abrams and S.H. Strogatz, “Chimera states for coupled oscillators,” *Physical review letters* **93**, 174102 (2004).
- [16] D. Domínguez and H.A. Cerdeira, “Order and turbulence in rf-driven josephson junction series arrays,” *Phys. Rev. Lett.* **71** (1993).
- [17] L.V. Gambuzza, A. Buscarino, S. Chessa, L. Fortuna, R. Meucci, and M. Frasca, “Experimental investigation of chimera states with quiescent and synchronous domains in coupled electronic oscillators,” *Phys. Rev. E* **9**, 032905 (2014).
- [18] L.V. Gambuzza, L. Minati, and M. Frasca, “Experimental observations of chimera states in locally and non-locally coupled stuart-landau oscillator circuits,” *Chaos, Solitons and Fractals* **138**, 109907 (2020).
- [19] A.M. Hagerstrom, T.E. Murphy, R. Roy, P. Hövel, I. Omelchenko, and E. Schöll, “Experimental observation of chimeras in coupled-map lattices,” *Nat. Phys.* **8**, 658–661 (2012).
- [20] E.A. Martens, S. Thutupalli, A. Fourriere, and O. Hallatschek, “Chimera states in mechanical oscillator networks,” *Proceedings of the National Academy of Sciences* **110**, 10563–10567 (2013).
- [21] M.H. Matheny, J. Emenheiser, W. Fon, A. Chapman, A. Salova, M. Rohden, J. Li, M. Hudoba de Badyn, M. Pósfai, L. Duenas-Ororio, M. Mesbahi, J.P. Crutchfield, M.C. Cross, R.M. D’Souza, and M.L. Roukes, “Exotic states in a simple

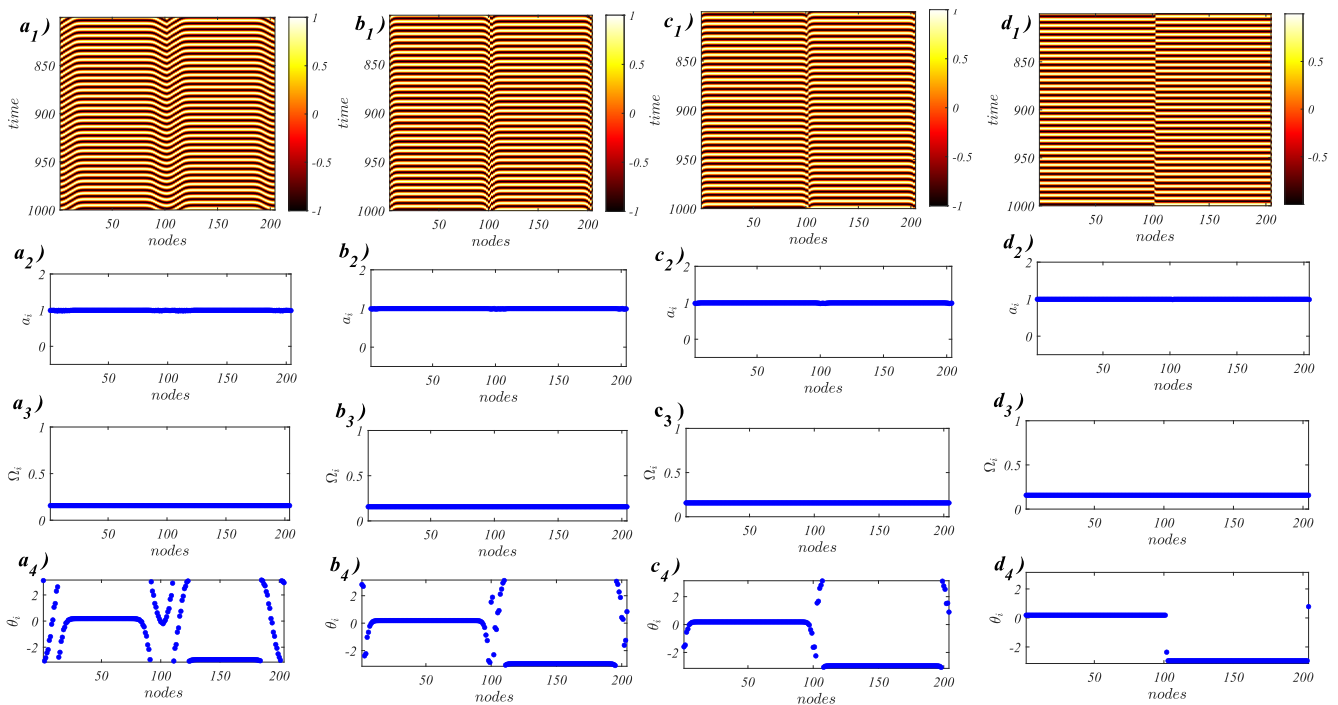


Figure A2. Analysis of the dynamics on a 2-directed 2-hypergraph of 204 nodes with a different orientation with respect to the Main Text. The first row shows the spatiotemporal diagrams, the second row the amplitudes, the third row the frequencies, and the last row the phases. The directionality parameter  $p$  is varied with the columns: (a1, a2, a3, a4) phase chimera state for  $p = 1$ ; (b1, b2, b3, b4) phase chimera state for  $p = 0.2$ ; (c1, c2, c3, c4) phase chimera state for  $p = 0.1$ ; (d1, d2, d3, d4) coherent clusters for  $p = 0$ . The model parameters are  $\alpha = 1$  and  $\omega = 1$ , and the coupling strength is  $\varepsilon = 0.02$ .

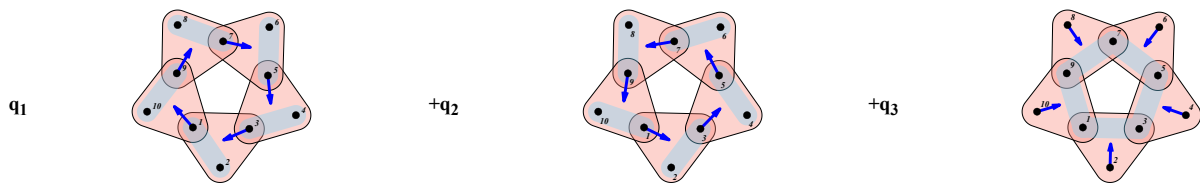


Figure B1. Schematically representation of a family of 2-directed 2-hypergraphs. In the graphical representation, the heads of the hyperedges are highlighted in blue, while arrows indicate the directionality of the connections between the nodes.

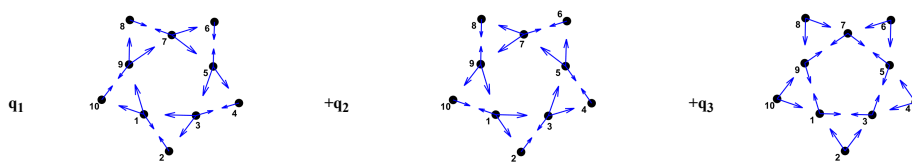


Figure B2. Schematic representation of a family of clique-projected networks, corresponding to the 2-directed 2-hypergraph of the previous Figure. Note that in the case of 2-directed 2-hypergraphs, the two head nodes interact with each other.

- network of nanoelectromechanical oscillators,” *Science* **363**, eaav7932 (2019).
- [22] A. Zakharova, *Chimera Patterns in Networks. Interplay between Dynamics, Structure, Noise, and Delay* (Springer, 2020).
- [23] F. Parastesh, S. Jafari, H. Azarnoush, Z. Shahriari, Z. Wang, S. Boccaletti, and M. Perc, “Chimeras,” *Physics Reports* **898**, 1–114 (2021).
- [24] T. Chouzouris, I. Omelchenko, A. Zakharova, J. Hlinka, P. Jiruska, and E. Schöll, “Chimera states in brain networks: Empirical neural vs. modular fractal connectivity,” *Chaos* **28**, 045112 (2018).
- [25] S. Majhi, B.K. Bera, D. Ghosh, and M. Perc, “Chimera states in neuronal networks: A review,” *Physics of life reviews* **28**, 100–121 (2019).

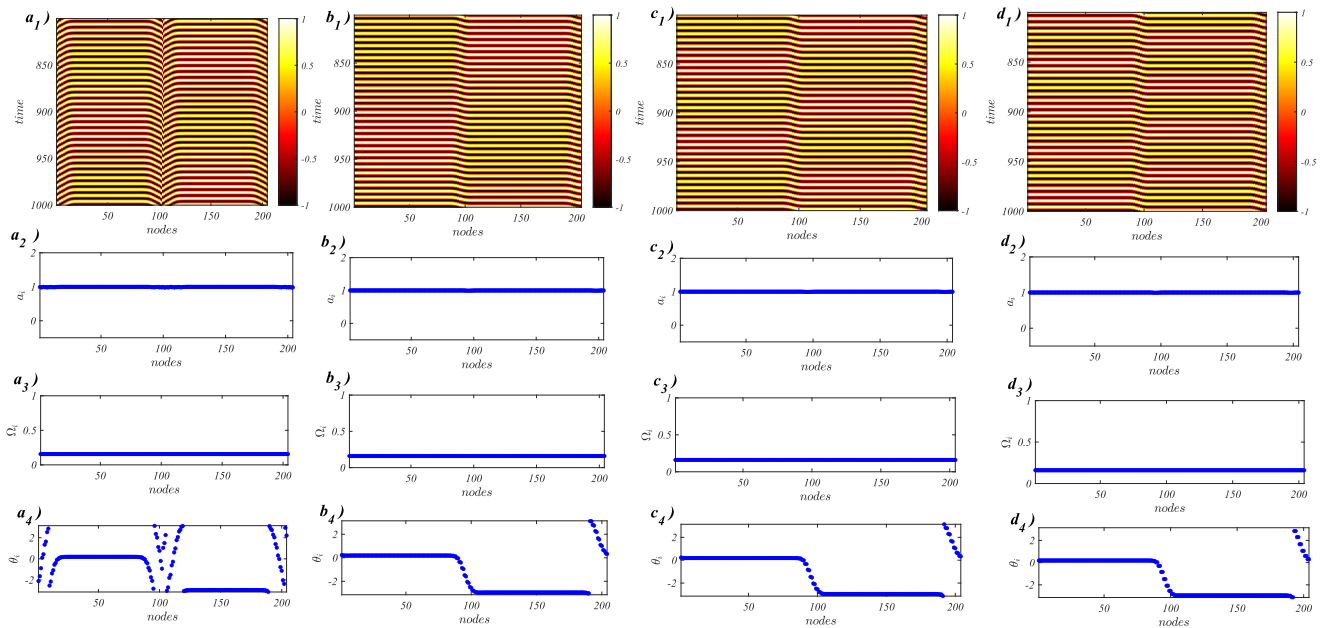


Figure B3. Analysis of the dynamics on a 2-directed 2-hypergraph of 204 nodes. The first row shows the spatiotemporal diagrams, the second row the amplitudes, the third row the frequencies, and the last row the phases. The directionality parameter  $p$  is varied with the columns: (a1, a2, a3, a4) phase chimera state for  $p = 1$  ; (b1, b2, b3, b4) coherent clusters for  $p = 0.2$  ; (c1, c2, c3, c4) coherent clusters for  $p = 0.1$  ; (d1, d2, d3, d4) coherent clusters for  $p = 0$ . The model parameters are  $\alpha = 1$  and  $\omega = 1$ , and the coupling strength is  $\varepsilon = 0.015$ .

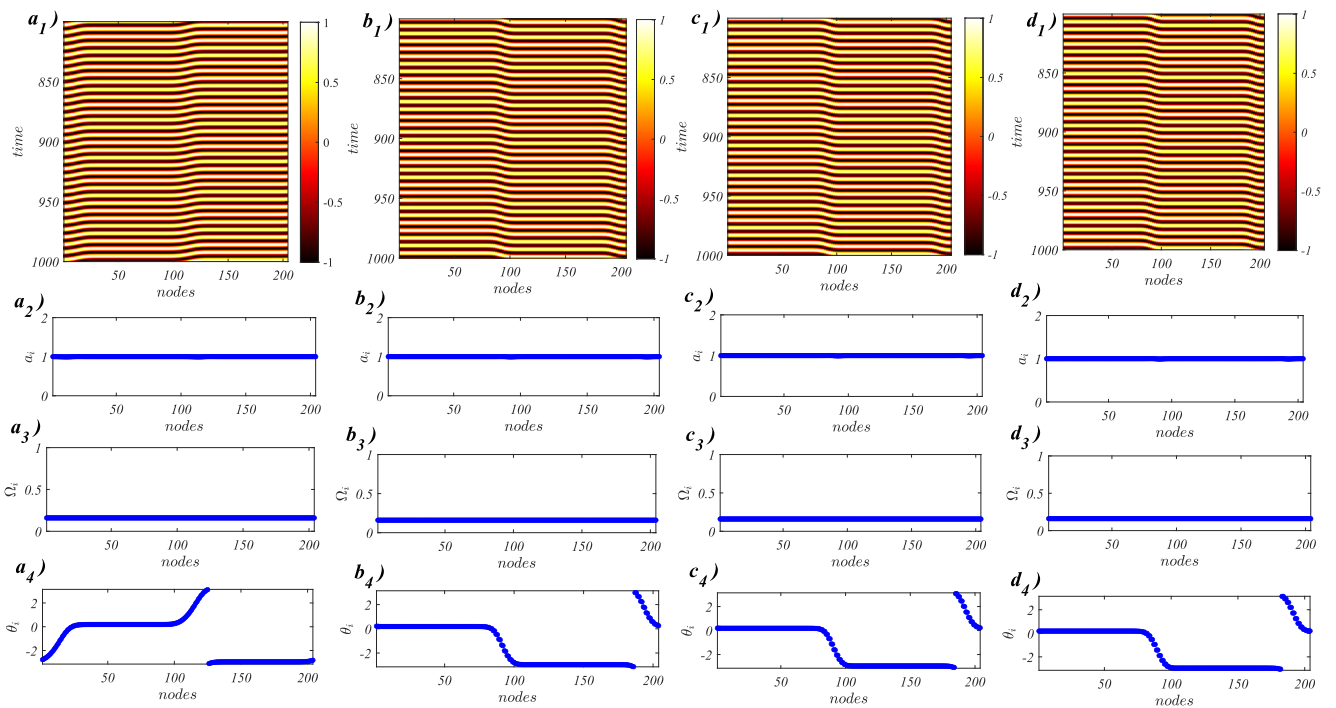


Figure B4. Analysis of the dynamics on a clique-projected network of 204 nodes. The first row shows the spatiotemporal diagrams, the second row the amplitudes, the third row the frequencies, and the last row the phases. The directionality parameter  $p$  is varied with the columns: (a1, a2, a3, a4) coherent clusters for  $p = 1$  ; (b1, b2, b3, b4) coherent clusters for  $p = 0.2$  ; (c1, c2, c3, c4) coherent clusters for  $p = 0.1$  ; (d1, d2, d3, d4) coherent clusters for  $p = 0$ . The model parameters are  $\alpha = 1$  and  $\omega = 1$ , and the coupling strength is  $\varepsilon = 0.015$ .

[26] N.C. Rattenborg, C.J. Amlaner, and S.L. Lima, “Behavioral, neurophysiological and evolutionary perspectives on unihemi-

spheric sleep,” *Neuroscience & Biobehavioral Reviews* **24**, 817–842 (2000).

- [27] M. Asllani, R. Lambiotte, and T. Carletti, “Structure and dynamical behavior of non-normal networks,” *Sci. Adv.* **4**, Eaa9403 (2018).
- [28] Christian Bick and Erik A Martens, “Controlling chimeras,” *New Journal of Physics* **17**, 033030 (2015).
- [29] Kris Vasudevan, Michael Cavers, and Antony Ware, “Earthquake sequencing: Chimera states with kuramoto model dynamics on directed graphs,” *Nonlinear Processes in Geophysics* **22**, 499–512 (2015).
- [30] Nicolás Deschle, Andreas Daffertshofer, Demian Battaglia, and Erik A Martens, “Directed flow of information in chimera states,” *Frontiers in Applied Mathematics and Statistics* **5**, 28 (2019).
- [31] P. Jaros, R. Levchenko, T. Kapitaniak, and Y. Maistrenko, “Chimera states for directed networks,” *Chaos* **31** (2021).
- [32] M. Asllani, B.A. Siebert, A. Arenas, and J.P. Gleeson, “Symmetry-breaking mechanism for the formation of cluster chimera patterns,” *Chaos* **32**, 013107 (2022).
- [33] R. Muolo, J.D. O’Brien, T. Carletti, and M. Asllani, “Persistence of chimera states and the challenge for synchronization in real-world networks,” *The European Physical Journal B* **97**, 6 (2024).
- [34] F. Battiston, G. Cencetti, I. Iacopini, V. Latora, M. Lucas, A. Patania, J.-G. Young, and G. Petri, “Networks beyond pairwise interactions: structure and dynamics,” *Phys. Rep.* (2020).
- [35] F. Battiston, E. Amico, A. Barrat, G. Bianconi, G. Ferraz de Arruda, B. Franceschiello, I. Iacopini, S. Kéfi, V. Latora, Y. Moreno, M.M. Murray, T.P. Peixoto, F. Vaccarino, and G. Petri, “The physics of higher-order interactions in complex systems,” *Nat. Phys.* **17**, 1093–1098 (2021).
- [36] G. Bianconi, *Higher-Order Networks: An introduction to simplicial complexes* (Cambridge University Press, 2021).
- [37] S. Boccaletti, P. De Lellis, C.I. Del Genio, K. Alfaro-Bittner, R. Criado, S. Jalan, and M. Romance, “The structure and dynamics of networks with higher order interactions,” *Physics Reports* **1018**, 1–64 (2023).
- [38] C. Bick, E. Gross, H.A. Harrington, and M.T. Schaub, “What are higher-order networks?” *SIAM Review* **65**, 686–731 (2023).
- [39] R. Muolo, L. Giambagli, H. Nakao, D. Fanelli, and T. Carletti, “Turing patterns on discrete topologies: from networks to higher-order structures,” *Proceedings of the Royal Society A* **480**, 20240235 (2024).
- [40] A.P. Millán, H. Sun, L. Giambagli, R. Muolo, T. Carletti, J.J. Torres, F. Radicchi, J. Kurths, and G. Bianconi, “Topology shapes dynamics of higher-order networks,” *Nat. Phys.* **21**, 353–361 (2025).
- [41] R.D. Andrew, M. Fagan, B.A. Ballyk, and A.S. Rosen, “Seizure susceptibility and the osmotic state,” *Brain Res.* **498**, 175–180 (2021).
- [42] M. Wang, D. Arteaga, and B.j. He, “Brain mechanisms for simple perception and bistable perception,” *Proc. Natl. Acad. Sci. U.S.A.* **110**, E3350–E3359 (2013).
- [43] G. Petri, P. Expert, F. Turkheimer, R. Carhart-Harris, D. Nutt, P.J. Hellyer, and F. Vaccarino, “Homological scaffolds of brain functional networks,” *J. Royal Soc. Interface* **11**, 20140873 (2014).
- [44] A.E. Sizemore, C. Giusti, A. Kahn, J.M. Vettel, R.F. Betzel, and D.S. Bassett, “Cliques and cavities in the human connectome,” *J. Comp. Neurosci.* **44**, 115–145 (2018).
- [45] J. Grilli, G. Barabás, M.J. Michalska-Smith, and S. Allesina, “Higher-order interactions stabilize dynamics in competitive network models,” *Nature* **548**, 210–213 (2017).
- [46] I. Iacopini, J.R. Foote, N.H. Fefferman, E.P. Derryberry, and M.J. Silk, “Not your private tête-à-tête: leveraging the power of higher-order networks to study animal communication,” *Phil. Trans. R. Soc. Lond. B* **379**, 20230190 (2024).
- [47] D. Centola, J. Becker, D. Brackbill, and A. Baronchelli, “Experimental evidence for tipping points in social convention,” *Science* **360**, 1116–1119 (2018).
- [48] T. Carletti, F. Battiston, G. Cencetti, and D. Fanelli, “Random walks on hypergraphs,” *Phys. Rev. E* **101**, 022308 (2020).
- [49] M.T. Schaub, A.R. Benson, P. Horn, G. Lippner, and A. Jadbabaie, “Random walks on simplicial complexes and the normalized Hodge 1-Laplacian,” *SIAM Rev.* **62**, 353–391 (2020).
- [50] T. Tanaka and T. Aoyagi, “Multistable attractors in a network of phase oscillators with three-body interactions,” *Phys. Rev. Lett.* **106**, 224101 (2011).
- [51] P.S. Skardal and A. Arenas, “Higher order interactions in complex networks of phase oscillators promote abrupt synchronization switching,” *Comm. Phys.* **3**, 1–6 (2020).
- [52] A.P. Millán, J.J. Torres, and G. Bianconi, “Explosive higher-order Kuramoto dynamics on simplicial complexes,” *Phys. Rev. Lett.* **124**, 218301 (2020).
- [53] L.V. Gambuzza, F. Di Patti, L. Gallo, S. Lepri, M. Romance, R. Criado, M. Frasca, V. Latora, and S. Boccaletti, “Stability of synchronization in simplicial complexes,” *Nat. Comm.* **12**, 1–13 (2021).
- [54] I. León, R. Muolo, S. Hata, and H. Nakao, “Higher-order interactions induce anomalous transitions to synchrony,” *Chaos* **34** (2024).
- [55] I. Iacopini, G. Petri, A. Barrat, and V. Latora, “Simplicial models of social contagion,” *Nat. Comm.* **10**, 2485 (2019).
- [56] L. DeVillie, “Consensus on simplicial complexes: Results on stability and synchronization,” *Chaos* **31**, 023137 (2021).
- [57] T. Carletti, D. Fanelli, and S. Nicoletti, “Dynamical systems on hypergraphs,” *J. phys. Complex.* **1**, 035006 (2020).
- [58] R. Muolo, L. Gallo, V. Latora, M. Frasca, and T. Carletti, “Turing patterns in systems with high-order interaction,” *Chaos Solit. Fractals* **166**, 112912 (2023).
- [59] S. Kundu and D. Ghosh, “Higher-order interactions promote chimera states,” *Physical Review E* **105**, L042202 (2022).
- [60] X. Li, D. Ghosh, and Y. Lei, “Chimera states in coupled pendulum with higher-order interactions,” *Chaos, Solitons and Fractals* **170**, 113325 (2023).
- [61] C. Bick, T. Böhle, and C. Kuehn, “Phase oscillator networks with nonlocal higher-order interactions: Twisted states, stability, and bifurcations,” *SIAM J. Appl. Dyn. Syst.* **22** (2023).
- [62] R. Muolo, T. Njougouo, L.V. Gambuzza, T. Carletti, and M. Frasca, “Phase chimera states on nonlocal hyperrings,” *Physical Review E* **109**, L022201 (2024).
- [63] R. Muolo, L.V. Gambuzza, H. Nakao, and M. Frasca, “Pinning control of chimera states in systems with higher-order interactions,” *arXiv preprint arXiv:2409.02658* (2024).
- [64] L. Gallo, R. Muolo, L.V. Gambuzza, V. Latora, M. Frasca, and T. Carletti, “Synchronization induced by directed higher-order interactions,” *Comm. Phys.* **5** (2022).
- [65] F. Della Rossa, D. Liuzza, F. Lo Iudice, and P. De Lellis, “Emergence and control of synchronization in networks with directed many-body interactions,” *Physical Review Letters* **131**, 207401 (2023).
- [66] M. Dorchain, W. Segnou, R. Muolo, and T. Carletti, “Impact of directionality on the emergence of turing patterns on m-directed higher-order structures,” *Chaos, Solitons & Fractals* **189**, 115730 (2024).
- [67] Gautam C Sethia, Abhijit Sen, and George L Johnston, “Amplitude-mediated chimera states,” *Physical Review E* **88**,

- 042917 (2013).
- [68] E.R. Zajdela and D.M. Abrams, “Phase chimera states: frozen patterns of disorder,” arXiv preprint arXiv:2308.06190 (2023).
- [69] H. Nakao, “Phase reduction approach to synchronisation of nonlinear oscillators,” *Contemporary Physics* **57**, 188–214 (2016).
- [70] Y. Kuramoto and H. Nakao, “On the concept of dynamical reduction: the case of coupled oscillators,” *Philosophical Transactions of the Royal Society A* **377**, 20190041 (2019).
- [71] C. Bick, T. Böhle, and O.E. Omel’chenko, “Hopf bifurcations of twisted states in phase oscillators rings with nonpairwise higher-order interactions,” arxiv preprint <https://arxiv.org/abs/2310.15698> (2023).
- [72] Yuanzhao Zhang, Per Sebastian Skardal, Federico Battiston, Giovanni Petri, and Maxime Lucas, “Deeper but smaller: Higher-order interactions increase linear stability but shrink basins,” *Science Advances* **10**, eado8049 (2024).
- [73] H. Nakao, “Complex ginzburg-landau equation on networks and its non-uniform dynamics,” *Eur. Phys. J. Spec. Top.* **223**, 2411–2421 (2014).
- [74] Y. Kuramoto, “Self-entrainment of a population of coupled non-linear oscillators,” in *International Symposium on Mathematical Problems in Theoretical Physics*, edited by Huzihiro Araki (Springer Berlin Heidelberg, Berlin, Heidelberg, 1975) pp. 420–422.
- [75] Y. Kuramoto, *Chemical oscillations, waves, and turbulence* (Springer-Verlag, New York, 1984).
- [76] Juan A Acebrón, Luis L Bonilla, Conrad J Pérez Vicente, Félix Ritort, and Renato Spigler, “The Kuramoto model: A simple paradigm for synchronization phenomena,” *Rev. Mod. Phys.* **77**, 137 (2005).
- [77] I. León and H. Nakao, “Analytical phase reduction for weakly nonlinear oscillators,” *Chaos, Solitons & Fractals* **176**, 114117 (2023).
- [78] P. Ashwin and A. Rodrigues, “Hopf normal form with sn symmetry and reduction to systems of nonlinearly coupled phase oscillators,” *Physica D: Nonlinear Phenomena* **325**, 14–24 (2016).
- [79] I. León and D. Pazó, “Phase reduction beyond the first order: The case of the mean-field complex ginzburg-landau equation,” *Physical Review E* **100**, 012211 (2019).
- [80] Iván León and Diego Pazó, “Enlarged Kuramoto model: Secondary instability and transition to collective chaos,” *Phys. Rev. E* **105**, L042201 (2022).
- [81] Arkady Pikovsky Erik T. K. Mau, Michael Rosenblum, “High-order phase reduction for coupled 2d oscillators,” *Chaos: An Interdisciplinary Journal of Nonlinear Science* **33**, 101101 (2023).
- [82] Iván L., R. Muolo, S. Hata, and H. Nakao, “Theory of phase reduction for systems with higher-order interactions: a route to kuramoto models on hypergraphs,” arXiv preprint arXiv:2503.21587 (2025).
- [83] P.S. Skardal and A. Arenas, “Abrupt desynchronization and extensive multistability in globally coupled oscillator simplexes,” *Phys. Rev. Lett.* **122**, 248301 (2019).
- [84] M. Lucas, G. Cencetti, and F. Battiston, “Multiorder laplacian for synchronization in higher-order networks,” *Phys Rev. Res.* **2**, 033410 (2020).
- [85] J.A. Sanders, F. Verhulst, and J. Murdock, *Averaging Methods in Nonlinear Dynamical Systems. Second Edition, Applied Mathematical Sciences vol. 59* (Springer-Verlag, 2007).
- [86] Hidetsugu Sakaguchi and Yoshiki Kuramoto, “A soluble active rotator model showing phase transitions via mutual entertainment,” *Progress of Theoretical Physics* **76**, 576–581 (1986).